Whereas the possible existence of a liquid-water ocean on Europa is plausible, the opposite is true for Callisto. Callisto consists of roughly equal amounts of rock and ice. It is not tidally heated, there is no geological evidence for significant endogenic modification of its surface, and gravity measurements by the Galileo spacecraft show only partial separation of the ice and rock in its interior[28]. These observations are consistent with little modification of Callisto since its accretion. We note that thermal models of Callisto give no hint of a subsurface liquid-water ocean[17]. Accretional and radiogenic heating are marginally able to separate the ice and rock inside Callisto, but the present gravitational evidence shows that unlike Ganymede[29] separation has been incomplete: Callisto has not been heated enough to have melted all its ice.

Is it possible for some of the ice in the outer part of Callisto to have melted, and could a near-surface liquid-water layer be prevented from freezing? Because accretional heating is largest when a planet is near maximum size, we consider that it is possible for the ice to have melted in the outer layers of Callisto. More problematic is keeping such a layer from freezing; tidal heating is necessary for the maintenance of a liquid ocean on Europa, and there is no tidal heating on Callisto. The presence of 'antifreeze' (salts or ammonia) would help. The layer needs to have substantial thickness, and for this reason an ocean separating two solid convecting regions is most plausible. The possibility of a liquid-water ocean in Callisto is startling, but we have no other explanation for the near-surface highly electrically conducting layer required by the observed induction signal. Of the two icy galilean satellites, it would be more plausible for Ganymede to have a subsurface liquid-water ocean. Ganymede is completely differentiated; extensive endogenic modification of its surface and the existence of an intrinsic magnetic field[3] imply a dynamic interior in the past, and possibly also in the present[30]. Perhaps Ganymede also has an internal liquid-water ocean if Callisto has one, but Ganymede's intrinsic magnetic field obscures any induction signal.

One possible source of heat not yet considered is ohmic heating by the eddy currents in the moons. The dissipated power can be estimated from the expression[31] power/area $= S\omega B^2/4\mu_o$, which is the ohmic loss from a propagating electromagnetic wave in a conducting waveguide (here μ_o is the permeability of vacuum). Multiplication by the surface area of the moon and substitution of varying field amplitudes of 220 nT (Europa) and 40 nT (Callisto) gives 5×10^6 (S/100 km) W for Europa and 4×10^5 (S/100 km) W for Callisto; nominal values for S are of the order of 100 km. More rigorous estimates would not change the conclusion that the heat input from this source is negligible.

We conclude from an analysis of the magnetic field observations that it is very likely that both Europa and Callisto possess internal salty liquid-water oceans. In the case of Europa, this conclusion is supported by indirect geological evidence[5,6]. □

Received 24 June; accepted 14 August 1998.

1. Kivelson, M. G. *et al*. Europa's magnetic signature: report from Galileo's first pass on December 19, 1996. *Science* **276,** 1239–1241 (1997).
2. Khurana, K. K., Kivelson, M. G., Russell, C. T., Walker, R. J. & Southwood, D. J. Absence of an internal magnetic field at Callisto. *Nature* **387,** 262–264 (1997).
3. Kivelson, M. G. Discovery of Ganymede's magnetic field by the Galileo spacecraft. *Nature* **384,** 537–541 (1996).
4. Kivelson, M. G. *et al*. A magnetic signature at Io: initial report from the Gallileo magnetometer. *Science* **273,** 337–340 (1996).
5. Carr, M. H. *et al*. Evidence for a subsurface ocean on Europa. *Nature* **391,** 363–365 (1998).
6. Pappalardo, R. T. *et al*. Geological evidence for solid-state convection in Europa's ice shell. *Nature* **391,** 365–368 (1998).
7. Parkinson, W. D. *Introduction to Geomagnetism* 308–340 (Scottish Academic, Edinburgh, 1993).
8. Neubauer, F. M. Nonlinear standing Alfvén wave current system at Io: Theory. *J. Geophys. Res.* **85,** 1171–1178 (1980).
9. Owen, C. J. *et al*. The lunar wake at 6.8 R_L: WIND magnetic field observations. *Geophys. Res. Lett.* **23,** 1263–1266 (1996).
10. Khurana, K. K. & Kivelson, M. G. Ultra low frequency MHD waves in Jupiter's middle magnetosphere. *J. Geophys. Res.* **94,** 5241–5254 (1989).
11. Ip, W-H. Europa's oxygen exosphere and its magnetospheric interaction. *Icarus* **120,** 317–325 (1996).
12. Kliore, A. J., Hinson, D. P., Flasar, F. M., Nagy, A. F. & Cravens, T. E. The ionosphere of Europa from Galileo radio occultations. *Science* **277,** 355–358 (1997).
13. Neubauer, F. M. The subalfvénic interaction of the Galilean satellites with the Jovian magnetosphere. *J. Geophys. Res. (Planets)* **103,** 19843–19866 (1998).
14. Montgomery, R. B. in *American Institute of Physics Handbook* 125–127 (McGraw Hill, New York, 1963).
15. Colburn, D. S. & Reynolds, R. T. Electrolytic currents in Europa. *Icarus* **63,** 39–44 (1985).
16. Kargel, J. S. & Consolmagno, G. J. Magnetic fields and the detectability of brine oceans in Jupiter's icy satellites. *Lunar Planet. Sci. Conf.* **XXVII,** 643–644 (1996).
17. Schubert, G., Spohn, T. & Reynolds, R. in *Satellites* (eds Burns, J. A. & Matthews, M. S.) 224–292 (Univ. Arizona Press, Tucson, 1986).
18. Anderson, J. D. Europa's differentiated internal structure: inferences from four Galileo encounters. *Science* (in the press).
19. Reynolds, R. T. & Cassen, P. On the internal structure of the major satellites of the outer planets. *Geophys. Res. Lett.* **6,** 121–124 (1979).
20. Kirk, R. L. & Stevenson, D. J. Thermal evolution of a differentiated Ganymede and implications for surface features. *Icarus* **69,** 91–135 (1987).
21. Cassen, P. M., Reynolds, R. T. & Peale, S. J. Is there liquid water on Europa? *Geophys. Res. Lett.* **6,** 731–734 (1979).
22. Squyres, S. W., Reynolds, R. T., Cassen, P. M. & Peale, S. J. Liquid water and active resurfacing on Europa. *Nature* **301,** 225–226 (1983).
23. Ross, M. N. & Schubert, G. Tidal heating in an internal ocean model of Europa. *Nature* **325,** 133–134 (1987).
24. Ojakangas, G. W. & Stevenson, D. J. Thermal state of an ice shell on Europa. *Icarus* **81,** 220–241 (1989).
25. Durham, W. B., Kirby, S. H. & Stern, L. A. Creep of water ices at planetary conditions: a compilation. *J. Geophys. Res.* **102,** 16293–16302 (1997).
26. McCord, T. B. *et al*. Salts on Europa's surface detected by Galileo's Near Infrared Mapping Spectrometer. *Science* **280,** 1242–1245 (1998).
27. Stevenson, D. J. in *Proc. Europa Conf.* 69–70 (San Juan Capistrano Research Inst., San Juan Capistrano, CA, 1996).
28. Anderson, J. D. *et al*. Distribution of rock, metals, and ices in Callisto. *Science* **280,** 1573–1576 (1998).
29. Anderson, J. D., Lau, E. L., Sjogren, W. L., Schubert, G. & Moore, W. B. Gravitational constraints on the internal structure of Ganymede. *Nature* **384,** 541–543 (1996).
30. Schubert, G., Zhang, K., Kivelson, M. G. & Anderson, J. D. The magnetic field and internal structure of Ganymede. *Nature* **384,** 544–545 (1996).
31. Jackson, J. D. *Classical Electrodynamics* 2nd edn 338 (Wiley, New York, 1975).
32. Connerney, J. E. P. Magnetic fields of the outer planets. *J. Geophys. Res.* **98,** 18659–18679 (1993).
33. Khurana, K. K. Euler potential models of Jupiter's magnetospheric field. *J. Geophys. Res.* **102,** 11295–11306 (1997).
34. M. G. Kivelson *et al*. Europa and Callisto; induced or intrinsic fields in a periodically varying plasma environment. *J. Geophys. Res.* (submitted).

Acknowledgements. We thank D. Bindschadler of the Jet Propulsion Laboratory for support in all phases of data collection and J. Mafi for data processing and preparation of data plots. This work was partially supported by the Jet Propulsion Laboratory.

Correspondence and requests for materials should be addressed to K.K.K. (e-mail: kkhurana@igpp.ucla.edu).

Quantized conductance through individual rows of suspended gold atoms

Hideaki Ohnishi*, Yukihito Kondo* & Kunio Takayanagi*†

** Takayanagi Particle Surface Project, ERATO, Japan Science and Technology Corporation, 3-1-2 Musashino, Akishima, Tokyo 196, Japan*
† Department of Material Science and Engineering, Tokyo Institute of Technology, 4259 Nagatsuta, Midori-ku, Yokohama, Kanagawa 226, Japan

As the scale of microelectronic engineering continues to shrink, interest has focused on the nature of electron transport through essentially one-dimensional nanometre-scale channels such as quantum wires[1] and carbon nanotubes[2,3]. Quantum point contacts (QPCs) are structures (generally metallic) in which a 'neck' of atoms just a few atomic diameters wide (that is, comparable to the conduction electrons' Fermi wavelength) bridges two electrical contacts. They can be prepared by contacting a metal surface with a scanning tunnelling microscope (STM)[4–7] and by other methods[8–12], and typically display a conductance quantized in steps of $2e^2/h(\sim 13\,k\Omega^{-1})$[13,14], where e is the electron charge and h is Planck's constant. Here we report conductance measurements on metal QPCs prepared with an STM that we can simultaneously image using an ultrahigh-vacuum electron microscope, which allows direct observation of the relation between electron transport and structure. We observe strands of gold atoms that are about one nanometre long and one single chain of gold atoms suspended between the electrodes. We can thus verify that the conductance of a single strand of atoms is $2e^2/h$ and that the conductance of a double strand is twice as large, showing that

equipartition holds for electron transport in these quantum systems.

Our miniaturized STM was placed at the specimen position of an ultrahigh-vacuum (UHV), high-resolution transmission electron microscope (TEM) which was equipped with a field emission gun operated at 200 kV. Operating this UHV TEM at 10^{-8} Pa allowed the clean fabrication of gold tips and samples *in situ*, thereby eliminating any effects of contamination on the structures and conductances.

A mechanically sharpened gold tip was positioned close to a gold island that had been deposited on a thin copper wire (the electrical connections are shown in Fig. 1). This gold tip could be displaced in three dimensions using a shear-type piezoelectric transducer. The gold tip was dipped into the gold island and slowly withdrawn at constant speed under computer control. Structural changes were observed continuously during withdrawal by means of a video monitor, and video images were recorded at 33-ms intervals; conductance was measured simultaneously. Stepped changes in conductance, corresponding to changes in the thickness of the gold bridge, were observed during withdrawal that were similar to those reported for STM experiments[4–7], a mechanically controllable break technique[8], pin-plate experiments[9] and switching electrodes[10–12].

Figure 2a–f shows electron microscope images of a gold bridge formed between the substrate and tip during withdrawal of the tip. The tip and substrate are oriented in the [110] direction and 0.2-nm spacings of the (200) lattice planes can be seen. The dark lines in the gold bridges represent rows of gold atoms spanning the distance from the substrate to the tip. The bridge thins in Fig. 2a–e and has broken in Fig. 2f; it appears to have reorganized itself into stable structures during withdrawal, with lines disappearing one-by-one, so that each bridge maintains a regular and uniform thickness. The structure of these thin gold bridges and their relation to conductance is a subject for future study. At this point, it should simply be noted that the lattice in Fig. 2a has a dislocation and that the gap between the dark lines of Fig. 2d is greatly enlarged relative to the (200) lattice spacings (0.2 nm) of the tip and substrate. The enlarged gap between the two rows is not an imaging artefact. We confirmed from the image simulation that TEM images reproduce the same gap distance as the model structure with two separate atomic rows (lattice planes).

More than 300 experiments provided clear evidence that linear strands of gold atoms make up the bridges and that the strands have a unit conductance of $2e^2/h$. Figure 3a shows the change in conductance during the withdrawal of an STM tip. The conductance was sampled at 33-ms intervals in order to coincide with the video frames. The conductance changed stepwise, with a step height corresponding to the unit conductance $G_0 = 2e^2/h$. TEM images corresponding to steps A and B in Fig. 3a are shown in the left and right panels of Fig. 3b, respectively. Both images show only a single dark line spanning the gap between the tip and the substrate. The fact that the conductance of step A was twice that of step B was explained by analysing the intensity profiles perpendicular to the bridges. As shown by the intensity profiles in Fig. 3c, the profile peak (hatched area) of the left bridge is twice the height of the right bridge. According to electron microscopy imaging theory[15], the peak height corresponds to the number of atoms stacked in the depth direction. We conclude that the right bridge in Fig. 3b is a single row of atoms having a unit conductance of $2e^2/h$ and that the left bridge contains two rows with a conductance equal to twice the unit conductance (corresponding models are shown in Fig. 3d).

We next investigated the structure of a bridge of atoms and of individual gold atoms arrayed in a linear strand (the electron microscope images the positions of the nuclei of the atoms). A very thin gold film was set in the specimen stage of the UHV electron microscope and bombarded with a very strong ($\sim$100 A cm^{-2}) electron beam in order to bore holes in the film. A free-standing nanobridge of gold was formed in vacuum by further thinning the material between adjacent holes. A nanobridge of 10 nm long and with four atomic rows (or planes) in its diameter was formed in the [110] direction of the (001) film[16]. From the (110) films, a single strand in the [001] direction frequently formed. This strand of atoms was often observed continuously for two minutes or more before breaking (a photograph of one such strand is shown in Fig. 4). Between the coloured edges of the gold film, four coloured dots corresponding to four gold atoms of the strand can be recognized. The gold atoms are spaced at 0.35–0.40 nm intervals which are much larger than the nearest-neighbour spacing (0.288 nm) of gold

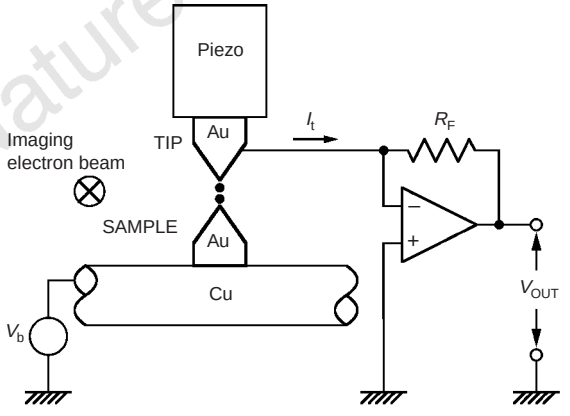

Figure 1 Scanning tunnelling microscope (STM) configuration built at the specimen stage of a UHV electron microscope. The conductance, $G = I_t/V_b$, was obtained by measuring $V_{out} = -R_F I_t$ for a constant bias voltage V_b, where R_F is the feedback resistor for current sensing, and I_t is the current passing through the contact between the tip and the sample. For most experiments, $V_b = 13$ mV and $R_F = 100$ kΩ. The imaging electron beam entered from top and typically had a current density of 0.45 fA nm^{-2} at the contact between the tip and the substrate. Bridges of gold atoms formed at the contact were imaged at $\times 10^7$ magnification on a video monitor and simultaneously recorded with the current at intervals of 33 ms.

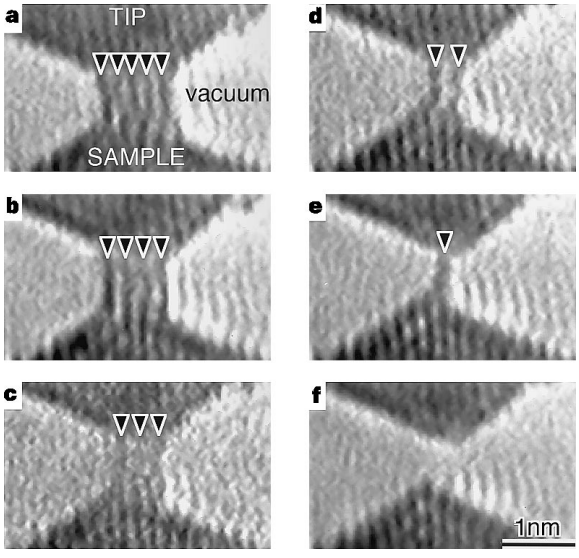

Figure 2 Electron microscope images of a contact while withdrawing the tip. A gold bridge formed between the gold tip (top) and gold substrate (bottom), thinned from **a** to **e** and ruptured at **f**, with observation times of 0, 0.47, 1.23, 1.33, 1.80 and 2.17 s, respectively. Dark lines indicated by arrowheads are rows of gold atoms. The faint fringe outside each bridge and remaining in **f** is a ghost due to interference of the imaging electrons. The conductance of the contact is 0 at **f** and $\sim 2 \times (13\,\text{k}\Omega)^{-1}$ at **e**. $V_b = -10$ mV and $R_F = 10$ kΩ.

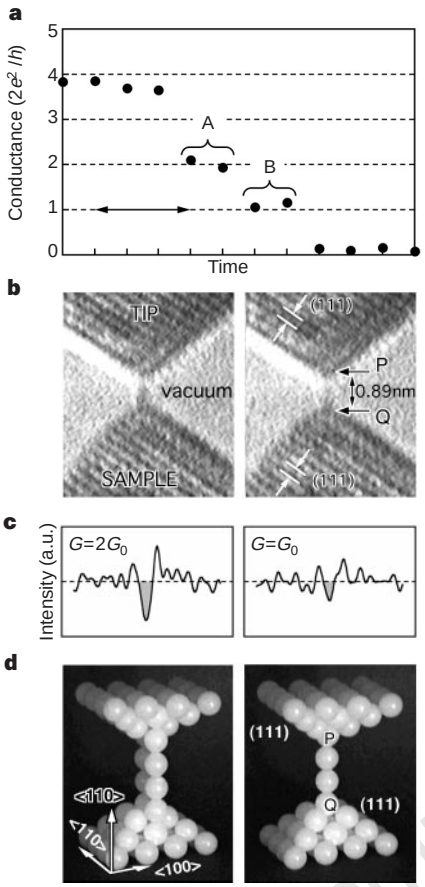

Figure 3 Quantized conductance of a single and a double strand of gold atoms. **a**, Conductance change of a contact while withdrawing the tip. Conductance is shown in units of $G_0 = 2e^2/h \sim (13\,\mathrm{k\Omega})^{-1}$. $V_b = +13$ mV and $R_F = 100\,\mathrm{k\Omega}$. **b**, Electron microscope images of gold bridges obtained simultaneously with the conductance measurements in **a**. Left, bridge at step A; right, bridge at step B. **c**, Intensity profiles of the left and right bridges shown in **b**. The shaded area is the intensity from the bridge after subtraction of the background noise. **d**, Models of the left and right bridges. The bridge at step A has two rows of atoms; the bridge at step B has only one row of atoms. The distance from P to Q (see **b**) is about 0.89 nm, wide enough to have two gold atoms in a bridge if the gold atoms have the nearest-neighbour spacing of the bulk crystal (0.288 nm).

atoms in the crystal.

The study of electron transport through point contacts in metals dates back to Maxwell's studies of the diffusive transport regime[17] and to Sharvin's proposal for the ballistic transport regime[18]. Quantization of conductance in the quantum mechanical ballistic regime was demonstrated experimentally for point contacts of two-dimensional GaAs–AlGaAs heterostructures[13,14] and for metal QPCs in the STM[4–7] and other geometries[8–12], and was explained by Landauer's formula[19] and Kubo's work[20]. Our result proves quantization of conductance for a linear strand of gold atoms. When a linear strand connects two reservoirs biased by $\mathrm{d}E(= eV_b)$ to produce a current $\mathrm{d}I(= I_t)$, then $\mathrm{d}I/\mathrm{d}E = 2e/h$. There are two foundations for this. First, electrons that move in a linear chain of gold atoms, with a momentum in the range $(p, p + \mathrm{d}p)$, can only carry a current of $\mathrm{d}I = 2e(\partial E/\partial p)(\mathrm{d}p/h) = (2e/h)\mathrm{d}E$, where $\partial E/\partial p$ is the velocity of the electron at the Fermi level and $\mathrm{d}p/h$ is the number of electrons, irrespective of the internal structure of the chain. Second, the number of allowable conduction channels, determined by the electron motion normal to the strand axis, is one for a single strand. The double strand, then, has twice the unit conductance if the interaction between the two individual rows is not strong.

The current atom bridges appear to differ from the QPCs in STM configurations[4–7]. For the QPCs, it is claimed that only narrow,

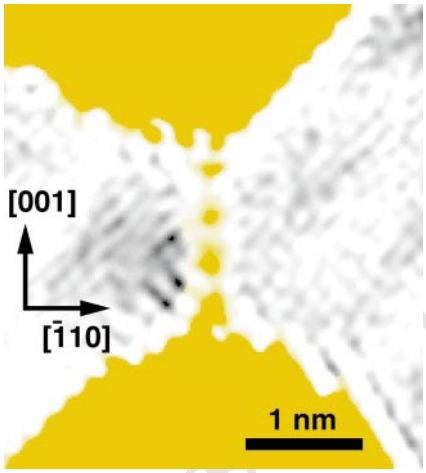

Figure 4 Electron microscope image of a linear strand of gold atoms (four coloured dots) forming a bridge between two gold films (coloured areas). The spacings of the four gold atoms are 0.35–0.40 nm. The strand is oriented along the [001] direction of the gold (110) film. This image was processed to highlight the linear strand, where the lattice fringes of the gold film in the original electron microscope image were filtered out by Fourier transform.

nanometre-wide necks form between tip and substrate. Molecular dynamics simulations[5,6,21,22] predict a narrow neck, but we did not find this here. A recent molecular dynamics simulation[23] reports elongated gold [110] and [001] wire structures in relation with the quantized conductance: the gold [110] wire (Fig. 8c of ref. 23) becomes permanently disordered, however; the [001] wire in Fig. 7c of ref. 23 is similar to the single atomic strand shown in our Fig. 4. This strand, however, has much larger atom spacings than those indicated by the molecular dynamics simulation. Regardless of the differences, some interesting issues remain to be investigated: the relation between the number of atomic rows in the strand and the number of channels for conducting electrons, quantum fluctuations of conductances that have been reported for metallic QPCs[7] and were also observed in the experiments described here following breakage of the strands, and the elementary excitation of conduction electrons in the strands.

The current linear strands persist for as long as two minutes. The gold strands in these experiments were stable, regular and uniform to an extent previously unrealized. The stability, regularity and uniformity of these strands of gold atoms are thought to be inherent to their natural, self-ordering phenomena, and may allow applications in devices as digitized units of electron conductors. □

Received 4 March; accepted 29 June 1998.

1. Webb, R. A., Washburn, S., Umbach, C. P. & Laibowitz, R. B. Observation of h/e Aharonov–Bohm oscillations in normal-metal rings. *Phys. Rev. Lett.* **54,** 2696–2699 (1985).
2. Iijima, S. Helical microtubules of graphitic carbon. *Nature* **354,** 56–58 (1991).
3. Bockrath, M. *et al.* Single-electron transport in ropes of carbon nanotubes. *Science* **275,** 1922–1925 (1997).
4. Agrait, N., Rodrigo, J. G. & Vieira, S. Conductance steps and quantization in atomic-size contacts. *Phys. Rev. B* **47,** 12345–12348 (1993).
5. Pascual, J. I. *et al.* Properties of metallic nanowires: from conductance quantization to localization. *Science* **267,** 1793–1795 (1995).
6. Olesen, L. *et al.* Quantized conductance in an atom-size point contact. *Phys. Rev. Lett.* **72,** 2251–2254 (1994).
7. Costa-Krämer, J. L. *et al.* Conductance quantization in nanowires formed between micro- and macroscopic metallic electrodes. *Phys. Rev. B* **55,** 5416–5424 (1997).
8. Muller, C. J., Krans, J. M., Todorov, T. N. & Reed, M. A. Quantization effects in the conductance of metallic contacts at room temperature. *Phys. Rev. B* **53,** 1022–1025 (1996).
9. Landman, U., Luedtke, W. D., Salisbury, B. E. & Whetten, R. L. Reversible manipulations of room-temperature mechanical and quantum transport properties in nanowire junctions. *Phys. Rev. Lett.* **77,** 1362–1365 (1996).
10. Costa-Krämer, J. L., García, N., García-Mochales, P. & Serena, P. A. Nanowire formation in macroscopic metallic contacts: quantum mechanical conductance tapping a table top. *Surf. Sci.* **342,** L1144–L1149 (1995).
11. Hansen, K., Lægsgaard, E., Stensgaard, I. & Besenbacher, F. Quantized conductance in relays. *Phys. Rev. B* **56,** 2208–2220 (1997).
12. Yasuda, H. & Sakai, A. Conductance of atomic-scale gold contacts under high-bias voltages. *Phys. Rev. B* **56,** 1069–1072 (1997).
13. van Wees, B. J. *et al.* Quantized conductance of point contacts in a two-dimensional electron gas. *Phys. Rev. Lett.* **60,** 848–850 (1988).

14. Wharam, D. A. *et al*. One-dimensional transport and the quantisation of the ballistic resistance. *J. Phys. C* **21,** L209–L214 (1988).
15. Cowley, J. M. in *Diffraction Physics* 62–63 (Elsevier, Amsterdam, 1975).
16. Kondo, Y. & Takayanagi, K. Gold nanobridge stabilized by surface structure. *Phys. Rev. Lett.* **79,** 3455–3458 (1997).
17. Maxwell, J. C. in *A Treatise on Electricity and Magnetism* (Clarendon, Oxford, 1904).
18. Sharvin, Y. V. A possible method for studying fermi surfaces. *Sov. Phys. JETP* **21,** 655–656 (1965).
19. Landauer, R. Spatial variation of currents and fields due to localized scatterers in metallic conduction. *IBM J. Rev. Dev.* **1,** 223–231 (1957).
20. Kubo, R. Statistical-mechanical theory of irreversible process. I. General theory and simple applications to magnetic and conduction problems. *J. Phys. Soc. Jpn* **12,** 570–586 (1957).
21. Landman, U., Luedtke, W. D., Burnham, N. A. & Colton, R. J. Atomic mechanics and dynamics of adhesion, nanoindentation, and fracture. *Science* **248,** 454–461 (1990).
22. Bratkovsky, A. M., Sutton, A. P. & Todorov, T. N. Conditions for conductance quantization in realistic models of atomic-scale metallic contacts. *Phys. Rev. B* **52,** 5036–5051 (1995).
23. Sørensen, M. R., Brandbyge, M. & Jacobsen, K. W. Mechanical deformation of atomic-scale metallic contacts: structure and mechanisms. *Phys. Rev. B* **57,** 3283–3294 (1998).

Correspondence and requests for materials should be addressed to H.O. (e-mail: ohnishi@tapro.jst.go.jp).

Formation and manipulation of a metallic wire of single gold atoms

A. I. Yanson*, G. Rubio Bollinger†, H. E. van den Brom*, N. Agraït† & J. M. van Ruitenbeek*

** Kamerlingh Onnes Laboratorium, Leiden University, PO Box 9504, NL-2300 RA Leiden, The Netherlands*
† Laboratorio de Bajas Temperaturas, Dept Física de la Materia Condensada C-III, Instituto Universitario de Ciencia de Materiales "Nicolás Cabrera", Universidad Autónoma de Madrid, E-28049 Madrid, Spain

The continuing miniaturization of microelectronics raises the prospect of nanometre-scale devices with mechanical and electrical properties that are qualitatively different from those at larger dimensions. The investigation of these properties, and particularly the increasing influence of quantum effects on electron transport, has therefore attracted much interest. Quantum properties of the conductance can be observed when 'breaking' a metallic contact: as two metal electrodes in contact with each other are slowly retracted, the contact area undergoes structural rearrangements until it consists in its final stages of only a few bridging atoms[1–3]. Just before the abrupt transition to tunnelling occurs, the electrical conductance through a monovalent metal contact is always close to a value of $2e^2/h$ ($\approx$12.9 kΩ^{-1}), where e is the charge on an electron and h is Planck's constant[4–6]. This value corresponds to one quantum unit of conductance, thus indicating that the 'neck' of the contact consists of a single atom[7]. In contrast to previous observations of only single-atom necks, here we describe the breaking of atomic-scale gold contacts, which leads to the formation of gold chains one atom thick and at least four atoms long. Once we start to pull out a chain, the conductance never exceeds $2e^2/h$, confirming that it acts as a one-dimensional quantized nanowire. Given their high stability and the ability to support ballistic electron transport, these structures seem well suited for the investigation of atomic-scale electronics.

The experimental techniques used for studies on metallic contacts of atomic dimensions are all based on piezoelectric transducers which allow fine positioning of two metal electrodes with respect to each other. Scanning tunnelling microscopy (STM), in which the tip is driven into contact with a metal surface and the conductance is measured during subsequent retraction, has been widely used for this purpose[4,5,8,9]. The other commonly used technique employs a mechanically controllable break-junction (MCB). In this case, one starts with a macroscopic notched wire[10], or a nanofabricated metal bridge[11] mounted on a flexible substrate. The wire (or bridge) is broken at low temperatures in vacuum, and contact is re-established between the fracture surfaces by piezoelectric control of substrate bending. Here we have used both MCB and a very stable STM at liquid-helium temperatures to produce and study chains of single gold atoms. In each case, high-purity (>99.99%) gold was used. Conductance was measured at a 10 mV d.c. voltage bias with 1% accuracy.

An example of a conductance curve obtained while stretching a gold nanocontact in an MCB is presented in Fig. 1. The curve reflects the evolution of some particular atomic configuration, during which the conductance decreases in a series of sharp vertically descending steps, with a gradual slope on the plateaux in between. These steps have been shown to be the result of atomic structural rearrangements[9,12]. The curves for successive rupture sequences do not repeat in detail, as they depend on the exact atomic positions in the contact. However, many curves have one striking feature in common: the remarkable length of the last conductance plateau just before rupture, at the value of about one conductance quantum, $G_0 = 2e^2/h$. Previous experiments have shown that the conductance at the last plateau for monovalent metals is usually close to 1 G_0 (refs 4–6), and it has been argued that these plateaux correspond to a contact with a single atom at the narrowest cross-section[7]. Examples have been found previously of exceptionally long stretched last plateaux, in particular for gold (see, for example, ref. 20), but this has not received due attention. The interest becomes clear when we recognize that the conductance of a point contact is determined predominantly by the size of its narrowest cross-section and that, during contact elongation, all structural transformations are localized to the neck region[2,3,12]. Figure 1 shows that during the last stage of elongation the conductance stays in a limited range of values corresponding to one atom in cross-section, while the contact is being stretched over distances up to 20 Å. This suggests the possibility that the contact stretches to form a chain of single atoms. As we cannot image the

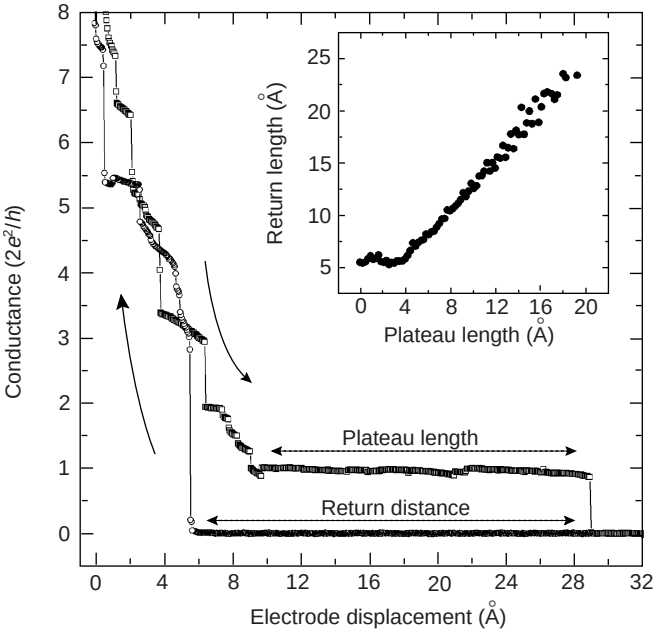

Figure 1 Conductance as a function of the displacement of the two gold electrodes with respect to each other in an MCB experiment at 4.2 K. The trace starts at the upper left, coming from higher conductance values (open squares). A long plateau with a conductance near 1 G_0 is observed and, after a jump to tunnelling, the electrode needs to return by a little more than the length of the long plateau to come back into contact (open circles). Inset, the average of the return distance as a function of the length of the long plateau (recorded with an STM at 4.2 K). The relation is approximately 1:1, with an offset of 5 Å which is probably due to the elasticity of the atomic structure.